The Exact Solution of the Falling Body Problem in Three-Dimensions: Comparative Study

Abdelhalim Ebaid [1],*, Weam Alharbi [1], Mona D. Aljoufi [1] and Essam R. El-Zahar [2,3],* ⓘD

[1] Department of Mathematics, Faculty of Science, University of Tabuk, Tabuk 71491,
Saudi Arabia; wgalharbi@ut.edu.sa (W.A.); maljufi@ut.edu.sa (M.D.A.)
[2] Department of Mathematics, Faculty of Sciences and Humanities in Al-Kharj,
Prince Sattam bin, Abdulaziz University, Al-Kharj 11942, Saudi Arabia
[3] Department of Basic Engineering Science, Faculty of Engineering, Menofia University,
Shebin El-Kom 32511, Egypt
* Correspondence: aebaid@ut.edu.sa (A.E.); er.elzahar@psau.edu.sa (E.R.E.-Z.);
Tel.: +966552884106 (A.E.); +966545046828 (E.R.E.-Z.)

✓ check for updates

Abstract: Very recently, the system of differential equations governing the three-dimensional falling body problem (TDFBP) has been approximately solved. The previously obtained approximate solution was based on the fact that the Earth's rotation (ER) is quite slow and hence all high order terms of ω in addition to the magnitude $\omega^2 R$ were neglected, where ω is the angular velocity and R is the radius of Earth. However, it is shown in this paper that the ignorance of such magnitudes leads, in many cases, to significant errors in the estimated falling time and other physical quantities. The current results are based on obtaining the exact solutions of the full TDFBP-system and performing several comparisons with the approximate ones in the relevant literature. The obtained results are of great interest and importance, especially for other planets in the Solar System or exterior planets, in which ω and/or $\omega^2 R$ are of considerable amounts and hence cannot be ignored. Therefore, the present analysis is valid in analyzing the TDFBP near to the surface of any spherical celestial body.

Keywords: falling body problem; angular velocity; projectile motion; three dimensions; Earth's rotation; Laplace transform

1. Introduction

In the past decades, some attention was given to the study of the falling body problem [1–3] and two-dimensional projectile motion [4–14]. In the literature [1–3], the falling body problem was modeled as the vertical motion of a particle near the Earth's gravitational field, i.e., as a problem formulated in one dimension. Hence, the results obtained in [1–3] and in [4–14] were only valid in a fixed frame, that is, a non-rotating one. By this, the effect of Earth's rotation (ER) on the falling body problem and also on the projectile motion was not considered. In addition, the effect of ER on the three dimensional-falling body problem (TDFBP) was analyzed very recently by El-Zahar et al. [15]. However, the analysis introduced by El-Zahar et al. [15] still has some restrictions where all high order terms of ω in addition to the magnitude $\omega^2 R$ were neglected. In this paper, we consider the effect of the ER on the TDFBP without any constraints/restrictions where all of the physical quantities are left arbitrary and therefore the present results generalize the previously published ones in [15]. The physical problem is described as follows. Let $\overrightarrow{r} = (x(t), y(t), z(t))$ be the position vector of a particle located at a point Q near the Earth's surface, relative to P (a surface point) as in Figure 1.
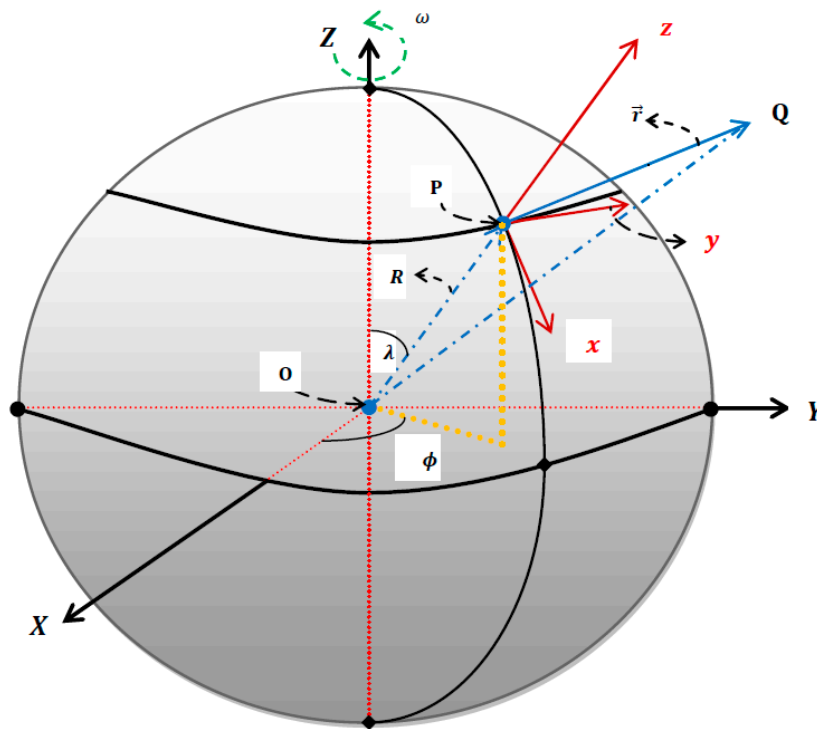
Figure 1. An inertial frame (X,Y,Z) attached to the centre of the Earth, and a point P on the surface, described by colatitude λ and longitude ϕ. The local Cartesian frame (x,y,z) at P. The x direction points south, the y direction points east, and the z direction points up. The position vector of a point Q relative to P is denoted $\vec{r}$.

The equations of motion in the frame (x, y, z) are given by [15–17]:

$$\ddot{x}(t) = (2\omega \cos \lambda)\dot{y}(t) + \omega^2(x(t) \cos \lambda + (R + z(t)) \sin \lambda) \cos \lambda, \tag{1}$$

$$\ddot{y}(t) = -(2\omega \cos \lambda)\dot{x}(t) - (2\omega \sin \lambda)\dot{z}(t) + \omega^2 y(t), \tag{2}$$

$$\ddot{z}(t) = -g + (2\omega \sin \lambda)\dot{y}(t) + \omega^2(x(t) \cos \lambda + (R + z(t)) \sin \lambda) \sin \lambda, \tag{3}$$

where g represents the acceleration due to gravity, ω denotes the Earth's angular velocity, $\lambda \in [0, \pi]$ is the colatitude, and R is the Earth's radius. Moreover, the x, y, and z directions points south, east, and up, respectively. Moreover, assume that a particle is released from rest at the point $Q = (x_0, y_0, z_0)$; hence, the initial conditions (ICs) are:

$$x(0) = x_0, \ y(0) = y_0, \ z(0) = z_0, \tag{4}$$

$$\dot{x}(0) = 0, \ \dot{y}(0) = 0, \ \dot{z}(0) = 0. \tag{5}$$

In the literature [15], system (1)–(4) has been approximately solved by neglecting all high order terms of ω in addition to the magnitude $\omega^2 R$. The present problem may be of practical importance in engineering and space sciences as explained below. Every day, many planes, satellites, and other space objects (such as the Mir Space Station and the International Space Station) orbit the Earth at different altitudes from the surface of the Earth. The Earth's planet is also exposed, annually, to many crashes of some aircrafts and meteorites, which cause a potential danger to vital installations and regions of population density in some countries. Therefore, the accurate identification of the possible location of

these falling objects clearly helps in the possibility of finding them successfully; hence, the importance of the current study. So, the objective of this paper is to solve the present system, taking into account the contributions of all terms without any constraints/restrictions on any of the physical quantities.

2. The Exact Solution

In this section, the exact solution of the full system (1)–(4) will be obtained without neglecting any of the higher orders of ω and also the magnitude $\omega^2 R$. The present approach implements the Laplace transform (LT) to exactly solving the full model (1)–(4). The Laplace transform and its properties are listed in Appendix A. Applying the LT on system (1)–(4) and in view of Equations (A4)–(A6), we have:

$$\left(s^2 - B\right)X(s) - CZ(s) - AsY(s) + \left(Ay_0 - x_0 s - \frac{CR}{s}\right) = 0, \tag{6}$$

$$\left(s^2 - \omega^2\right)Y(s) + AsX(s) + DsZ(s) - (Ax_0 + y_0 s + Dz_0) = 0, \tag{7}$$

$$\left(s^2 - E\right)Z(s) - CX(s) - DsY(s) + \left(\frac{g - ER}{s} - z_0 s + Dy_0\right) = 0, \tag{8}$$

where:

$$A = 2\omega \cos \lambda, \quad B = \omega^2 \cos^2 \lambda, \quad C = \omega^2 \sin \lambda \cos \lambda, \tag{9}$$

$$D = 2\omega \sin \lambda, \quad E = \omega^2 \sin^2 \lambda, \tag{10}$$

and $X(s)$, $Y(s)$, and $Z(s)$ are the LT of $x(t)$, $y(t)$, and $z(t)$, respectively. Solving system (6)–(8) for $X(s)$, $Y(s)$, and $Z(s)$, and implementing (9)–(10), we obtain:

$$X(s) = \frac{2x_0 s^6 + (\omega^2 k_1)s^4 + (4\omega^3 y_0 \cos \lambda)s^3 + \omega^2(\omega^2 k_2 + 3g \sin 2\lambda)s^2 + (\omega^4 g \sin 2\lambda)}{2s^3(s^2 + \omega^2)^2}, \tag{11}$$

$$Y(s) = \frac{y_0 s^3 + (3\omega^2 y_0)s + \omega k_3}{(s^2 + \omega^2)^2}, \tag{12}$$

$$Z(s) = \frac{z_0 s^6 + k_4 s^4 + (2\omega^3 y_0 \sin \lambda)s^3 + (\omega^2 k_5)s^2 - (\omega^4 g \cos^2 \lambda)}{s^3(s^2 + \omega^2)^2}, \tag{13}$$

where:

$$k_1 = (R + z_0) \sin 2\lambda + (5 + \cos 2\lambda)x_0, \tag{14}$$

$$k_2 = \omega^2(6x_0 - k_1), \tag{15}$$

$$k_3 = -2\omega^2 x_0 \cos \lambda - 2\left(-g + \omega^2(z_0 + R)\right) \sin \lambda, \tag{16}$$

$$k_4 = -g + \omega^2\left(R \sin^2 \lambda + \frac{1}{2}x_0 \sin 2\lambda + \frac{1}{2}z_0(5 - \cos 2\lambda)\right), \tag{17}$$

$$k_5 = 3\omega^2 z_0 - 3g \cos^2 \lambda - k_4. \tag{18}$$

Applying the inverse LT on (11)–(13), we obtain the explicit forms of $x(t)$, $y(t)$, and $z(t)$ as:

$$x(t) = \frac{1}{4\omega^2}\Big[2\omega^2 k_2 + g\big(2 + \omega^2 t^2\big)\sin 2\lambda\Big] + \frac{1}{4\omega}\Big[4\omega y_0 \cos \lambda + \big(\omega^2(k_1 - k_2 - 2x_0) - 2g\sin 2\lambda\big)t\Big]\times$$
$$\sin \omega t - \frac{1}{2\omega^2}\Big[\omega^2(k_2 - 2x_0) + g\sin 2\lambda + \big(2\omega^3 y_0 \cos \lambda\big)t\Big]\cos \omega t, \tag{19}$$

$$y(t) = \left(y_0 - \frac{k_3 t}{2\omega}\right)\cos \omega t + \left(\omega y_0 t + \frac{k_3}{2\omega^2}\right)\sin \omega t, \tag{20}$$

$$z(t) = \frac{1}{4\omega^2}\Big[4k_5 + 2g(4 - \omega^2 t^2)\cos^2 \lambda\Big] - \frac{1}{\omega^2}\Big[k_5 + 2g\cos^2 \lambda - \omega^2 z_0 + \big(\omega^3 y_0 \sin \lambda\big)t\Big]\cos \omega t -$$
$$\frac{1}{4\omega}\Big[-4\omega y_0 \sin \lambda + 2\big(k_5 - k_4 + \omega^2 z_0 + g\cos^2 \lambda\big)t\Big]\sin \omega t. \tag{21}$$

Equations (19)–(21) express the solution of the TDFBP model (1)–(4) without any assumptions or restrictions on ω and $\omega^2 R$. Expanding $x(t)$, $y(t)$, and $z(t)$ in (19)–(21) as power series in ω, yields:

$$x(t) = x_0 + \frac{t^2}{8}\cos \lambda\Big(4x_0 \cos \lambda + \big(gt^2 + 4z_0 + 4R\big)\sin \lambda\Big)\omega^2 + \left(\frac{t^3}{3}y_0 \cos \lambda\right)\omega^3 + \ldots, \tag{22}$$

$$y(t) = y_0 + \left(\frac{gt^3}{3}\sin \lambda\right)\omega + \left(\frac{y_0 t^2}{2}\right)\omega^2 - \frac{t^3}{30}\Big(10x_0 \cos \lambda + \big(gt^2 + 10z_0 + 10R\big)\sin \lambda\Big)\omega^3 + \ldots, \tag{23}$$

$$z(t) = \left(z_0 - \frac{gt^2}{2}\right) + \frac{t^2}{8}\sin \lambda\Big(4x_0 \cos \lambda + \big(gt^2 + 4z_0 + 4R\big)\sin \lambda\Big)\omega^2 + \left(\frac{y_0 t^3}{3}\sin \lambda\right)\omega^3 + \ldots. \tag{24}$$

As $\omega^2 \to 0$, the results (22)–(24) reduce to:

$$x(t) = x_0, \quad y(t) = y_0 + \left(\frac{gt^3}{3}\sin \lambda\right)\omega, \quad z(t) = z_0 - \frac{gt^2}{2}, \tag{25}$$

which are the corresponding results obtained in [15] when higher powers of ω, i.e., $\omega^n \ \forall \ n \geq 2$, are neglected. Furthermore, as $\omega^2 \to 0$, the horizontal and vertical displacements $x(t)$ and $z(t)$, respectively, are independent of the angular velocity ω. Moreover, Equations (22)–(24) reduce to some useful results at several special cases as declared in the subsequent sections.

3. Coordinates and Characteristics of the Falling Point

3.1. Coordinates of the Falling Point

Let G be the point at which the falling body hits the xy-plane, see Figure 2. At such point, the vertical displacement $z(t)$ vanishes. Suppose that T is the time required such that $z(T) = 0$; then, the Cartesian coordinates of the falling point G in the local frame (x, y, z) can be expressed as $(x_G, y_G, z_G) = (x(T), y(T), 0)$. In addition, the Polar coordinates (ρ, δ) of G are:

$$\rho = \sqrt{(x(T))^2 + (y(T))^2}, \quad \delta = \tan^{-1}\left(\frac{y(T)}{x(T)}\right). \tag{26}$$

In Appendix C, the coordinates of the falling point at various special cases are introduced.
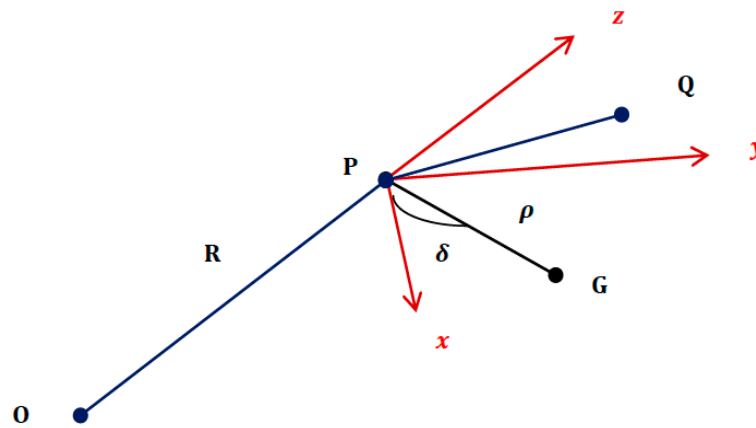
Figure 2. The particle, at rest, released from Q in the local Cartesian frame (x, y, z) hits the xy- plane at a point G. The angle between PG and the x-axis is denoted δ.

3.2. Characteristics of the Falling Point

In this section, we highlight some of the characteristics of the particle's falling point G. In particular, G lies on the Earth's surface when some conditions are satisfied. As $\rho \to 0$, G belongs to the Earth's surface, as shown from Figure 2. However, $\rho \to 0$ implies $x_G = y_G = 0$. The following lemmas address these issues.

Lemma 1. *If the particle is released from a point $(0, 0, z_0)$ in the system (x, y, z) such that $\lambda \in \{0, \pi\}$, then G belongs to the Earth's surface.*

Proof of Lemma 1. Substituting $x_0 = 0$ and $y_0 = 0$ into (19)–(21) and implementing the corresponding k_i $(i = 1, 2, 3, 4, 5)$ in (14)–(18), we have:

$$x(t) = \frac{\sin 2\lambda}{4\omega^2} [2(g - \omega^4(z_0 + R))(1 - \cos \omega t) + \omega(-2g + \omega^2(1 + \omega^2)(z_0 + R))t \, \sin \omega t + \omega^2 g t^2], \tag{27}$$

$$y(t) = \frac{\sin \lambda}{\omega^2}(g - \omega^4(z_0 + R))(\sin \omega t - \omega t \cos \omega t), \tag{28}$$

$$z(t) = \frac{1}{2\omega^2}[g - \omega^2(R - z_0) - \omega^2 g t^2 \cos^2 \lambda - (g - \omega^2(z_0 + R))(\cos 2\lambda + 2\sin^2 \lambda \times (\cos \omega t + \omega t \sin \omega t))]. \tag{29}$$

At such point G, the component $z(t)$ vanishes at a particular value $t = T$. Hence, x_G and y_G are, respectively, given from (27) and (28) by

$$x_G = \frac{\sin 2\lambda}{4\omega^2} [2(g - \omega^4(z_0 + R))(1 - \cos \omega T) + \omega(-2g + \omega^2(1 + \omega^2)(z_0 + R))T \sin \omega T + \omega^2 g T^2], \tag{30}$$

$$y_G = \frac{\sin \lambda}{\omega^2}(g - \omega^4(z_0 + R))(\sin \omega T - \omega T \cos \omega T), \tag{31}$$

where T is a non-trivial solution of the following equation $(z(T) = 0)$:

$$g - \omega^2(R - z_0) - \omega^2 g T^2 \cos^2 \lambda - (g - \omega^2(z_0 + R))(\cos 2\lambda + 2\sin^2 \lambda(\cos \omega T + \omega T \sin \omega T)). \tag{32}$$

It is clear from Equations (30) and (31) that $x_G = y_G = 0$ when $\sin 2\lambda = 0$ and $\sin \lambda = 0$. These two equations imply that $\lambda \in \{0, \pi\}$ which completes the proof. In addition, Equation (29) reduces to:

$$2z_0 - gT^2 = 0 \text{ which gives } T = \sqrt{\frac{2z_0}{g}}. \tag{33}$$

As a confirmation of this Lemma, we have from Appendix C (1 and 2) that $\rho = \sqrt{(1 + \omega^2 T^2)(x_0^2 + y_0^2)}$ for $\lambda = 0$ or π. When $(x_0, y_0) \to (0,0)$, we observe that $\rho \to 0$; hence, G lies on the Earth's surface. $\square$

Lemma 2. *If $x_0 = 0$ and $y_0 = 0$, then the falling point G is equivalent to the North Pole and the South Pole of Earth when $\lambda = 0$ and $\lambda = \pi$, respectively.*

Proof of Lemma 2. Let us first introduce the relation between the systems (x, y, z) and (X, Y, Z) described in Figure 1. It was shown in [16,17] that the following transformations hold after a time t:

$$X(t) = x(t) \cos \lambda \cos \omega t - y(t) \sin \omega t + (R + z(t)) \sin \lambda \cos \omega t, \tag{34}$$

$$Y(t) = x(t) \cos \lambda \sin \omega t + y(t) \cos \omega t + (R + z(t)) \sin \lambda \sin \omega t, \tag{35}$$

$$Z(t) = -x(t) \sin \lambda + (R + z(t)) \cos \lambda. \tag{36}$$

From Lemma 1, it was proved that $T = \sqrt{\frac{2z_0}{g}}$ when $x_0 = y_0 = 0$ and $\lambda \in \{0, \pi\}$, where G $= (x_G, y_G, z_G) = (0,0,0)$ in the local frame (x, y, z). Accordingly, the Cartesian coordinates (X_G, Y_G, Z_G) of G in the inertial frame (X, Y, Z) are:

$$X_G = x_G \cos \lambda \cos\left(\omega \sqrt{\frac{2z_0}{g}}\right) - y_G \sin\left(\omega \sqrt{\frac{2z_0}{g}}\right) + (R + z_G) \sin \lambda \cos\left(\omega \sqrt{\frac{2z_0}{g}}\right), \tag{37}$$

$$Y_G = x_G \cos \lambda \sin\left(\omega \sqrt{\frac{2z_0}{g}}\right) + y_G \cos = \left(\omega \sqrt{\frac{2z_0}{g}}\right) + (R + z_G) \sin \lambda \sin\left(\omega \sqrt{\frac{2z_0}{g}}\right), \tag{38}$$

$$Z_G = -x_G \sin \lambda + (R + z_G) \cos \lambda. \tag{39}$$

Substituting $x_G = y_G = z_G = 0$ into Equations (37)–(39) yields:

$$X_G = R \sin \lambda \cos\left(\omega \sqrt{\frac{2z_0}{g}}\right), \tag{40}$$

$$Y_G = R \sin \lambda \sin\left(\omega \sqrt{\frac{2z_0}{g}}\right), \tag{41}$$

$$Z_G = R \cos \lambda. \tag{42}$$

At $\lambda = 0$, we obtain:

$$X_G = 0, \quad Y_G = 0, \quad Z_G = R, \tag{43}$$

which are the Cartesian coordinates of the North pole in the frame (X, Y, Z). Moreover, we have from Equations (40)–(42) at $\lambda = \pi$ that:

$$X_G = 0, \quad Y_G = 0, \quad Z_G = -R, \tag{44}$$

which are equivalent to the Cartesian coordinates of the South Pole. □

4. Results and Discussions

This section presents the main difference between the current exact results and those approximately obtained by El-Zahar et al. [15]. Besides, the two Lemmas presented in the previous section will be numerically and graphically validated in this discussion. First of all, the falling time T is approximately obtained in [15] by $T_{\text{Approx.}} = \sqrt{\frac{2z_0}{g}}$ ∀ $\lambda \in [0, \pi]$. At $\lambda = 0, \pi$, it is noted from Appendix C (1 and 2) that the falling time T is obtained by $T = \sqrt{\frac{2z_0}{g}}$ which agrees with the corresponding expression in [15]. In such special cases, there is no difference between the current exact formula of the falling time T and the corresponding approximate one in [15]. However, when λ takes other values, i.e., $\lambda \in (0, \pi)$, there are differences in the calculations of T. In these cases, the exact values of T (T_{Exact}) can be calculated by solving Equation (21) as $z(T_{\text{Exact}}) = 0$; hence, the error formula of T is defined as:

$$\text{Error}(T) = T_{\text{Exact}} - \sqrt{\frac{2z_0}{g}}. \tag{45}$$

Table 1 presents the comparisons between the current values of the falling time T and the corresponding results in [15] at twenty different cases of the colatitude λ and the release point Q. The results reveal that the obtained error increases as the colatitude λ increases, especially at the equator of the Earth ($\lambda = \pi/2$). In [15], the approximate Cartesian coordinates $(x_G)_{\text{Approx.}}$ and $(y_G)_{\text{Approx.}}$ of the falling point G were given by:

$$(x_G)_{\text{Approx.}} = x_0, \quad (y_G)_{\text{Approx.}} = y_0 + \left(\frac{\omega g}{3}\right)\left(\sqrt{\frac{2z_0}{g}}\right)^3 \sin \lambda, \tag{46}$$

and the approximate polar coordinates $(\rho)_{\text{Approx.}}$ and $(\delta)_{\text{Approx.}}$ of G were obtained as [15]:

$$(\rho)_{\text{Approx.}} = \sqrt{x_0^2 + \left(y_0 + \left(\frac{\omega g}{3}\right)\left(\sqrt{\frac{2z_0}{g}}\right)^3 \sin \lambda\right)^2}, \tag{47}$$

$$(\delta)_{\text{Approx.}} = \tan^{-1}\left(\left(3y_0 + \omega g\left(\sqrt{\frac{2z_0}{g}}\right)^3 \sin \lambda\right) / 3x_0\right). \tag{48}$$

Table 1. Comparisons between the present values of the falling time (*T*) (s) and the corresponding results in [15] at various values of the colatitude (λ) (radian) and the release point Q.

Case	Colatitude (λ) (Radian)	Cartesian Coordinates of the Release Point Q			Falling Time (*T*) (S)		
		x_0 (km)	y_0 (km)	z_0 (km)	Exact (Present)	Approximate [15]	Error
1	$\pi/6$	10	10	10	45.1949	45.1754	0.0195
2	$\pi/6$	20	20	20	63.9154	63.8877	0.0277
3	$\pi/6$	30	30	30	78.2803	78.2461	0.0342
4	$\pi/6$	40	40	40	90.3905	90.3508	0.0397
5	$\pi/6$	50	50	50	101.0598	101.0153	0.0445
6	$\pi/4$	10	10	10	45.2145	45.1754	0.0391
7	$\pi/4$	20	20	20	63.9431	63.8877	0.0554
8	$\pi/4$	30	30	30	78.3143	78.2461	0.0682
9	$\pi/4$	40	40	40	90.4299	90.3508	0.0791
10	$\pi/4$	50	50	50	101.1040	101.0153	0.0887
11	$\pi/3$	10	10	10	45.2340	45.1754	0.0586
12	$\pi/3$	20	20	20	63.9708	63.8877	0.0831
13	$\pi/3$	30	30	30	78.3483	78.2461	0.1022
14	$\pi/3$	40	40	40	90.4692	90.3508	0.1184
15	$\pi/3$	50	50	50	101.1480	101.0153	0.1327
16	$\pi/2$	10	10	10	45.2535	45.1754	0.0781
17	$\pi/2$	20	20	20	63.9984	63.8877	0.1107
18	$\pi/2$	30	30	30	78.3820	78.2461	0.1359
19	$\pi/2$	40	40	40	90.5082	90.3508	0.1574
20	$\pi/2$	50	50	50	101.1916	101.0153	0.1763

Therefore, the errors in x_G, y_G, ρ, and δ at $\lambda = 0$ are given by:

$$\text{Error}(x_G) = \left(x_0 - \omega y_0 \sqrt{\frac{2z_0}{g}}\right)\cos\left(\omega\sqrt{\frac{2z_0}{g}}\right) + \left(y_0 + \omega x_0 \sqrt{\frac{2z_0}{g}}\right)\sin\left(\omega\sqrt{\frac{2z_0}{g}}\right) - x_0, \tag{49}$$

$$\text{Error}(y_G) = \left(y_0 + \omega x_0 \sqrt{\frac{2z_0}{g}}\right)\cos\left(\omega\sqrt{\frac{2z_0}{g}}\right) - \left(x_0 - \omega y_0 \sqrt{\frac{2z_0}{g}}\right)\sin\left(\omega\sqrt{\frac{2z_0}{g}}\right) - y_0, \tag{50}$$

$$\text{Error}(\rho) = \sqrt{(1 + \omega^2 T^2)(x_0^2 + y_0^2)} - \sqrt{x_0^2 + y_0^2}, \tag{51}$$

$$\text{Error}(\delta) = \tan^{-1}\left(\frac{\left(y_0 + \omega x_0\sqrt{\frac{2z_0}{g}}\right)\cos\left(\omega\sqrt{\frac{2z_0}{g}}\right) - \left(x_0 - \omega y_0\sqrt{\frac{2z_0}{g}}\right)\sin\left(\omega\sqrt{\frac{2z_0}{g}}\right)}{\left(x_0 - \omega y_0\sqrt{\frac{2z_0}{g}}\right)\cos\left(\omega\sqrt{\frac{2z_0}{g}}\right) + \left(y_0 + \omega x_0\sqrt{\frac{2z_0}{g}}\right)\sin\left(\omega\sqrt{\frac{2z_0}{g}}\right)}\right) - \tan^{-1}\left(\frac{y_0}{x_0}\right). \tag{52}$$

Similarly, at $\lambda = \pi$, we have:

$$\text{Error}(x_G) = \left(x_0 + \omega y_0 \sqrt{\frac{2z_0}{g}}\right)\cos\left(\omega\sqrt{\frac{2z_0}{g}}\right) - \left(y_0 - \omega x_0 \sqrt{\frac{2z_0}{g}}\right)\sin\left(\omega\sqrt{\frac{2z_0}{g}}\right) - x_0, \tag{53}$$

$$\text{Error}(y_G) = \left(y_0 - \omega x_0 \sqrt{\frac{2z_0}{g}}\right)\cos\left(\omega\sqrt{\frac{2z_0}{g}}\right) + \left(x_0 + \omega y_0 \sqrt{\frac{2z_0}{g}}\right)\sin\left(\omega\sqrt{\frac{2z_0}{g}}\right) - y_0, \tag{54}$$

$$\text{Error}(\rho) = \sqrt{(1 + \omega^2 T^2)(x_0^2 + y_0^2)} - \sqrt{x_0^2 + y_0^2}, \tag{55}$$

$$\text{Error}(\delta) = \tan^{-1}\left(\frac{\left(y_0-\omega x_0\sqrt{\frac{2z_0}{g}}\right)\cos\left(\omega\sqrt{\frac{2z_0}{g}}\right)+\left(x_0+\omega y_0\sqrt{\frac{2z_0}{g}}\right)\sin\left(\omega\sqrt{\frac{2z_0}{g}}\right)}{\left(x_0+\omega y_0\sqrt{\frac{2z_0}{g}}\right)\cos\left(\omega\sqrt{\frac{2z_0}{g}}\right)-\left(y_0-\omega x_0\sqrt{\frac{2z_0}{g}}\right)\sin\left(\omega\sqrt{\frac{2z_0}{g}}\right)}\right)- \\ \tan^{-1}\left(\frac{y_0}{x_0}\right). \tag{56}$$

Table 2 presents the obtained errors in the Cartesian coordinates of the falling point $G(x_G, y_G, 0)$ in the frame (x, y, z) and the corresponding errors in the Polar coordinates (ρ, δ) at several points $Q(x_0, y_0, z_0)$ when $\lambda = 0, \pi$. The results of Table 2 indicate that the obtained errors in ρ and δ are of the amount at $\lambda = 0$ (North Pole) and $\lambda = \pi$ (South Pole). In addition, the errors increase as the height z_0 increases above the Earth's surface. While the obtained errors in ρ and δ in Table 2 seem very small at these particular values of the colatitude λ, it will be declared that the errors in x_G and y_G, ρ, and δ are significant at other values of $\lambda \in (0, \pi)$. Repeating the analysis above at $\lambda = \pi/6$, $\lambda = \pi/4$, $\lambda = \pi/3$, and $\lambda = \pi/2$, we calculated the errors of x_G and y_G, as introduced in Table 3.

Table 2. The obtained errors of the Cartesian coordinates of the falling point $G(x_G, y_G, 0)$ in the frame (x, y, z) and the corresponding errors in the polar coordinates (ρ, δ) at several points $Q(x_0, y_0, z_0)$ when $\lambda = 0, \pi$.

Case	Colatitude (λ) (Radian)	Cartesian Coordinates of the Release Point Q			Error of Cartesian Coordinates of G			Error of Polar Coordinates of G	
		x_0 (km)	y_0 (km)	z_0 (km)	Error of x_G (m)	Error of y_G (m)	Error of ρ	Error of δ ($\times 10^{-8}$)(Radian)
1	0	10	10	10	0.0541	0.0538	0.0763	1.1819
2	0	20	20	20	0.2165	0.2152	0.3053	3.3429
3	0	30	30	30	0.4875	0.4838	0.6868	6.1413
4	0	40	40	40	0.8672	0.8596	1.2211	9.4550
5	0	50	50	50	1.3557	1.3425	1.9079	13.2137
6	π	10	10	10	0.2152	0.0541	0.0763	1.1819
7	π	20	20	20	0.4838	0.2165	0.3053	3.3429
8	π	30	30	30	0.8596	0.4875	0.6868	6.1413
9	π	40	40	40	1.3425	0.8672	1.2211	9.4550
10	π	50	50	50	0.2152	1.3557	1.9079	13.2137

Table 3. The obtained errors of x_G and y_G at several release points $Q(x_0, y_0, z_0)$ when $\lambda = \pi/6, \pi/4, \pi/3, \pi/2$.

Case	Colatitude (λ) (Radian)	Cartesian Coordinates of the Release Point Q			Error of Cartesian Coordinates of G	
		x_0 (km)	y_0 (km)	z_0 (km)	Error of x_G (m)	Error of y_G (m)
1	$\pi/6$	10	10	10	14.9922	0.0303
2	$\pi/6$	20	20	20	30.1361	0.1487
3	$\pi/6$	30	30	30	45.4317	0.3619
4	$\pi/6$	40	40	40	60.8793	0.6722
5	$\pi/6$	50	50	50	76.4789	1.0808
6	$\pi/4$	10	10	10	17.3067	0.0407
7	$\pi/4$	20	20	20	34.7489	0.1782
8	$\pi/4$	30	30	30	52.3271	0.4166
9	$\pi/4$	40	40	40	70.0412	0.7570
10	$\pi/4$	50	50	50	87.8912	1.2004
11	$\pi/3$	10	10	10	14.9911	0.0623
12	$\pi/3$	20	20	20	30.0799	0.2398
13	$\pi/3$	30	30	30	45.2667	0.5302
14	$\pi/3$	40	40	40	60.5515	0.9327
15	$\pi/3$	50	50	50	75.9343	1.4469
16	$\pi/2$	10	10	10	4.8873×10^{-8}	21.9937
17	$\pi/2$	20	20	20	3.9099×10^{-7}	62.2715
18	$\pi/2$	30	30	30	1.3196×10^{-6}	114.4901
19	$\pi/2$	40	40	40	3.1280×10^{-6}	176.3861
20	$\pi/2$	50	50	50	6.1094×10^{6}	246.6514

The results show that the errors in x_G and y_G increases as λ, x_0, y_0, and z_0 increase. For example, when the release point $Q(x_0, y_0, z_0)$ takes the values $Q(10,10,10)$, the errors in x_G are found as 14.9922 m at $\lambda = \pi/6$, 17.3067 m at $\lambda = \pi/4$, 75.9343 m at $\lambda = \pi/3$. However, the obtained maximum errors in y_G are 1.4469 m when $\lambda = \pi/3$. Moreover, at $\lambda = \pi/2$ (the equator of Earth), the obtained errors in x_G are small for the five cases of $Q(x_0, y_0, z_0)$, while the obtained error in y_G becomes significant and considerable, equaling 246.6514 m for $Q(50,50,50)$. Of course, the significant errors in the Cartesian coordinates x_G and in y_G imply significant errors in the polar coordinates ρ and in δ. The above calculations implemented the real data of the Earth's planet and can also be extended to cover other planets in the Solar System. Finally, the advantage of the present analysis over the previously published one is observable, especially when applied to specific planets of greater radius R and greater angular velocity ω than those of the Earth.

In order to confirm such conclusion, the current exact solutions are applied for all planets in our Solar System, Mercury, Venus, Earth, Mars, Jupiter, Saturn, Uranus, and Neptune. Astronomers usually divide the planets into two groups, which are known as the inner planets (Mercury, Venus, Earth, and Mars) and the outer planets (Jupiter, Saturn, Uranus, and Neptune) [18]. It will be indicated below that the obtained errors for the falling time T and the landing positions $(x_G, y_G, 0)$ are bigger for the outer planets than those of the inner planets.

In Table 4, the physical data for all planets are introduced. Before launching to the main results, it can be seen from Table 4 that the value of angular velocity ω of any outer planet (Jupiter, Saturn, Uranus, and Neptune) is greater than the value of any inner planet. This means that the outer planets rotate more speedily about their axes than the inner planets. In another word, the Coriolis effect is expected to affect the calculated errors for outer planets more than it does for the inner planets. In addition, the radii of the outer planets are greater than the radii of the inner planets. So, it is expected that the differences between the present exact solutions and the approximate ones [15] will greatly appear in the cases of outer planets.

Table 4. Data for the planets in the Solar System [18].

Planet	Ratio of Acceleration Due to Gravity [Earth = 1]	Acceleration Due to Gravity [m/s²]	Radius (km)	Rotation Period (in Earth Days)	Angular Velocity [s⁻¹]
Mercury	0.38	3.7278	2439	58.65	1.24×10^{-6}
Venus	0.9	8.829	6052	243	2.99×10^{-7}
Earth	1	9.80	6378	1.00	7.27×10^{-5}
Mars	0.38	3.7278	3394	1.03	7.10×10^{-5}
Jupiter	2.64	25.8984	71,400	0.41	1.80×10^{-4}
Saturn	0.93	9.1233	60,000	0.44	1.70×10^{-4}
Uranus	0.89	8.7309	25,559	0.72	1.0×10^{-4}
Neptune	1.12	10.9872	24,764	0.72	1.0×10^{-4}

Our point of view can be confirmed through the calculations in Tables 5 and 6 for $\lambda = \pi/6$ and $\lambda = \pi/4$, respectively. Such calculations are based on assuming that a projectile, at rest, is released from the point $Q(50,50,50)$. The results in Tables 5 and 6 reveal that the obtained errors of T for outer planets are greater than those of inner ones. In addition, for the obtained errors of y_G, although small for all planets, we find that the corresponding errors of x_G are significant, especially, for those outer planets. Therefore, the current exact analysis may be more helpful than the approximate one, particularly when studying the falling body problem near to the surface of a planet with greater values of ω and R than those of Earth, as it already appeared in cases of Jupiter, Saturn, Uranus, and Neptune. Finally, we are in a period of new planets, new space bodies. For this reason, the current results may also be valid for new planets, which may be discovered later.

Table 5. The obtained errors of the falling time T, x_G, and y_G for all planets in the Solar System at the release point Q(50,50,50) (km) when $\lambda = \pi/6$.

Planet	Errors of Falling Time (*T*) [S]	Errors of x_G and y_G	
		Error of x_G (m)	Error of y_G (m)
Mercury	0.000022	0.02334	0.00103
Venus	0.000020	0.00714	0.00003
Earth	0.044593	76.48	1.08084
Mars	0.098546	104.25	2.80507
Jupiter	0.707271	1982.68	7.62458
Saturn	2.586710	4332.41	29.9594
Uranus	0.396289	642.56	0.43672
Neptune	0.271695	493.98	0.01481

Table 6. The obtained errors of the falling time T, x_G, and y_G for all planets in the Solar System at the release point Q(50,50,50) (km) when $\lambda = \pi/4$.

Planet	Errors of Falling Time (*T*) [S]	Errors of x_G and y_G	
		Error of x_G (m)	Error of y_G (m)
Mercury	0.00004	0.02637	0.00103
Venus	0.00001	0.00153	0.00003
Earth	0.08874	87.8912	1.20038
Mars	0.19522	119.268	3.06653
Jupiter	1.43850	2341.8	3.25094
Saturn	5.37170	5262.61	16.1197
Uranus	0.79587	746.424	0.99274
Neptune	0.54491	572.814	0.99814

5. Conclusions

In this paper, the three dimensional model of the falling body problem near the Earth's surface was analyzed, taking into account the contribution of all physical quantities. Moreover, unlike the previous published paper [15], the values of the involved parameters were left arbitrary without any restrictions/constraints. Thus, the exact solutions of the full-three coupled equations of motion were obtained in terms of the release point $Q(x_0, y_0, z_0)$, the colatitude λ, the angular velocity ω, and the radius R of Earth. The present analysis was based on the Laplace transform as a method of solution. Furthermore, the properties of the falling point in the rotating frame and the original inertial frame were given by means of two lemmas. In addition, the conditions at which the falling point belongs $G = (x_G, y_G, z_G)$ to the Earth's surface were theoretically proven. The effectiveness and validity of the present analysis over the published one in the literature [15] arises when applied to other planets of greater radius R and angular velocity ω than those of the Earth. Hence, the present analysis is applicable to analyzing the TDFBP near enough to the surface of any spherical celestial body.

Appendix A

Laplace Transform and Its Properties

The LT of a function $u(t)$ is defined as [19]

$$L\{u(t)\} = \int_0^\infty e^{-st} u(t) dt = U(s),$$ (A1)

where the LT of $u(t)$ is said to exist if the integral (A1) converges. The sufficient conditions for existence of the LT are detailed in [8], see pages (1–2). Moreover, the LT of the n-derivative of $u(t)$ is given by [19].

$$L\{u^{(n)}(t)\} = s^n U(s) - \sum_{m=0}^{n-1} s^{n-m-1} u^{(m)}(0).$$ (A2)

For $n = 2$, we have

$$L\{\ddot{u}(t)\} = s^n U(s) - su(0) - \dot{u}(0).$$ (A3)

Applying the last formula on $\ddot{x}(t)$, $\ddot{y}(t)$, and $\ddot{z}(t)$, yields

$$L(\ddot{x}(t)) = s^2 X(s) - sx(0) - \dot{x}(0),$$ (A4)

$$L(\ddot{y}(t)) = s^2 Y(s) - sy(0) - \dot{y}(0),$$ (A5)

$$L(\ddot{z}(t)) = s^2 Z(s) - sz(0) - \dot{z}(0),$$ (A6)

Appendix B

Appendix B.1. Special Cases

Appendix B.1.1. $\lambda = 0$ (North Pole)

At $\lambda = 0$, we have from (14)–(18) the following values for k_i, $i = 1,2,3,4,5$:

$$k_1 = 6x_0, \ k_2 = 0, \ k_3 = -2\omega^2 x_0, \ k_4 = -g + 2\omega^2 z_0, \ k_5 = -2g + \omega^2 z_0.$$ (A7)

Substituting (26) into (22)–(24), we obtain

$$x(t) = (x_0 - \omega y_0 t) \cos \omega t + (y_0 + \omega x_0 t) \sin \omega t,$$ (A8)

$$y(t) = (y_0 + \omega x_0 t) \cos \omega t - (x_0 - \omega y_0 t) \sin \omega t,$$ (A9)

$$z(t) = z_0 - \frac{gt^2}{2}.$$ (A10)

It is noted from these equations that only $z(t)$ is independent of the angular velocity ω.

Appendix B.1.2. $\lambda = \pi$ (South Pole)

In this case, we have

$$k_1 = 6x_0, \ k_2 = 0, \ k_3 = 2\omega^2 x_0, \ k_4 = -g + 2\omega^2 z_0, \ k_5 = -2g + \omega^2 z_0. \tag{A11}$$

Accordingly, Equations (22)–(24) become

$$x(t) = (x_0 + \omega y_0 t) \cos \omega t - (y_0 - \omega x_0 t) \sin \omega t, \tag{A12}$$

$$y(t) = (y_0 - \omega x_0 t) \cos \omega t + (x_0 + \omega y_0 t) \sin \omega t, \tag{A13}$$

$$z(t) = z_0 - \frac{gt^2}{2}. \tag{A14}$$

Equation (A14) indicates that $z(t)$ is not influenced by ω as in the previous special case.

Appendix B.1.3. $\lambda = \frac{\pi}{2}$ (Equator)

At $\lambda = \frac{\pi}{2}$ and proceeding as above, we have

$$k_1 = 4x_0, \ k_2 = 2\omega^2 x_0, \ k_3 = 2g - 2\omega^2(z_0 + R), \tag{A15}$$

$$k_4 = -g + \omega^2(3z_0 + R), \ k_5 = g - \omega^2 R, \tag{A16}$$

and

$$x(t) = \omega^2 x_0 + \left(1 - \omega^2\right)x_0 \cos \omega t + \frac{1}{2}\omega\left(1 - \omega^2\right)x_0 t \sin \omega t, \tag{A17}$$

$$y(t) = \frac{1}{\omega}\left[\omega y_0 - \left(g - \omega^2(z_0 + R)\right)t\right]\cos \omega t + \frac{1}{\omega^2}\left[\omega^3 y_0 t + \left(g - \omega^2(z_0 + R)\right)\right]\sin \omega t, \tag{A18}$$

$$z(t) = \frac{g - \omega^2 R}{\omega^2} + \frac{1}{\omega^2}\left[-g + \omega^2(z_0 + R) - \omega^3 y_0 t\right]\cos \omega t + \frac{1}{\omega}\left[\omega y_0 + \left(-g + \omega^2(z_0 + R)\right)t\right]\sin \omega t. \tag{A19}$$

Here, it can be seen from Equations (A17)–(A19) that ω is involved in all the components $x(t)$, $y(t)$, and $z(t)$.

Appendix C

Appendix C.1. Coordinates of the Falling Point at Special Cases

Appendix C.1.1. $\lambda = 0$ (North Pole)

From (A10), by solving the equation $z(T) = 0$ for T, we obtain

$$T = \sqrt{\frac{2z_0}{g}}. \tag{A20}$$

Hence, x_G and y_G are given from (B.2,3) by

$$x_G = (x_0 - \omega y_0 T) \cos \omega T + (y_0 + \omega x_0 T) \sin \omega T, \tag{A21}$$

$$y_G = (y_0 + \omega x_0 T) \cos \omega T - (x_0 - \omega y_0 T) \sin \omega T. \tag{A22}$$

From Equatios (26), we have

$$\rho = \sqrt{(1 + \omega^2 T^2)(x_0^2 + y_0^2)}, \tag{A23}$$

$$\delta = \tan^{-1}\left(\frac{(y_0 + \omega x_0 T) \cos \omega T - (x_0 - \omega y_0 T) \sin \omega T}{(x_0 - \omega y_0 T) \cos \omega T + (y_0 + \omega x_0 T) \sin \omega T}\right), x_0 \neq 0, y_0 \neq 0. \tag{A24}$$

Appendix C.1.2. $\lambda = \pi$ (South Pole)

In this case, we have

$$x_G = (x_0 + \omega y_0 T) \cos \omega T - (y_0 - \omega x_0 T) \sin \omega T, \tag{A25}$$

$$y_G = (y_0 - \omega x_0 T) \cos \omega T + (x_0 + \omega y_0 T) \sin \omega T, \tag{A26}$$

where T is defined by (C.1) and consequently

$$\rho = \sqrt{(1 + \omega^2 T^2)(x_0^2 + y_0^2)}, \tag{A27}$$

$$\delta = \tan^{-1}\left(\frac{(y_0 - \omega x_0 T) \cos \omega T + (x_0 + \omega y_0 T) \sin \omega T}{(x_0 + \omega y_0 T) \cos \omega T - (y_0 - \omega x_0 T) \sin \omega T}\right), x_0 \neq 0, y_0 \neq 0. \tag{A28}$$

Appendix C.1.3. $\lambda = \frac{\pi}{2}$ (Equator)

In the previous cases, the time T was explicitly obtained as seen from (C.1). However, the present case is different and requires solving the following implicit equation in T:

$$\frac{g - \omega^2 R}{\omega^2} + \frac{1}{\omega^2}\left[-g + \omega^2(z_0 + R) - \omega^3 y_0 T\right] \cos \omega T + \frac{1}{\omega}\left[\omega y_0 + \left(-g + \omega^2(z_0 + R)\right)T\right] \sin \omega T = 0, \tag{A29}$$

which can be simplified as

$$(g - \omega^2 R) + \left[-g + \omega^2(z_0 + R) - \omega^3 y_0 T\right] \cos \omega T + \omega\left[\omega y_0 + \left(-g + \omega^2(z_0 + R)\right)T\right] \sin \omega T = 0. \tag{A30}$$

The corresponding x_G and y_G are given as and

$$x_G = \omega^2 x_0 + \left(1 - \omega^2\right)x_0 \cos \omega T + \frac{1}{2}\omega\left(1 - \omega^2\right)x_0 T \sin \omega T, \tag{A31}$$

$$y_G = \frac{1}{\omega}\left[\omega y_0 - \left(g - \omega^2(z_0 + R)\right)T\right] \cos \omega T + \frac{1}{\omega^2}\left[\omega^3 y_0 T + \left(g - \omega^2(z_0 + R)\right)\right] \sin \omega T. \tag{A32}$$

Hence

$$\rho = \sqrt{x_G^2 + y_G^2}, \tag{A33}$$

$$\delta = \tan^{-1}\left(\frac{\omega\left[\omega y_0 - \left(g - \omega^2(z_0 + R)\right)T\right]\cos\omega T + \left[\omega^3 y_0 T + \left(g - \omega^2(z_0 + R)\right)\right]\sin\omega T}{\omega^4 x_0 + \omega^2(1 - \omega^2)x_0\cos\omega T + \frac{1}{2}\omega^3(1 - \omega^2)x_0 T\sin\omega T}\right), \tag{A34}$$

where $x \neq 0$.

References

1. Kwok, S.F. A falling body problem through the air in view of the fractional derivative approach. *Phys. A Stat. Mech. Appl.* **2005**, *350*, 199–206.
2. Garcia, J.J.R.; Calderon, M.G.; Ortiz, J.M.; Baleanu, D.; de Santiago, C.S.V. Motion of a particle in a resisting medium using fractional calculus approach. *Proc. Rom. Acad. A* **2013**, *14*, 42–47.
3. Ebaid, A.; Masaedeh, B.; Machado, J.A.T. A New Fractional Model for the Falling Body Problem. *Chin. Phys. Lett.* **2017**, *34*, 20201. [CrossRef]
4. Hayen, J.C. Projectile motion in a resistant medium: Part I: Exact solution and properties. *Int. J. Non-linear Mech.* **2003**, *38*, 357–369. [CrossRef]
5. Hayen, J.C. Projectile motion in a resistant medium Part II: Approximate solution and estimates. *Int. J. Non-linear Mech.* **2003**, *38*, 371–380. [CrossRef]
6. Weinacht, P.; Cooper, G.R.; Newell, J.F. *Analytical Prediction of Trajectories for High-Velocity Direct-Fire Munitions*; Technical report ARL-TR-3567; US Army Research Laboratory: Aberdeen Proving Ground, MD, USA, 2005.
7. Yabushita, K.; Yamashita, M.; Tsuboi, K. An analytic solution of projectile motion with the quadratic resistance law using the homotopy analysis method. *J. Phys. A Math. Theor.* **2007**, *40*, 8403–8416. [CrossRef]
8. Benacka, J. Solution to projectile motion with quadratic drag and graphing the trajectory in spreadsheets. *Int. J. Math. Educ. Sci. Technol.* **2010**, *41*, 373–378. [CrossRef]
9. Benacka, J. On high-altitude projectile motion. *Can. J. Phys.* **2011**, *89*, 1003–1008. [CrossRef]
10. Ebaid, A. Analysis of projectile motion in view of fractional calculus. *Appl. Math. Model.* **2011**, *35*, 1231–1239. [CrossRef]
11. Rosales, J.J.; Guía, M.; Gómez, F.; Aguilar, F.; Martinez, J. Two dimensional fractional projectile motion in a resisting medium. *Open Phys.* **2014**, *12*, 517–520. [CrossRef]
12. Ahmad, B.; Batarfi, H.; Nieto, J.J.; Otero-Zarraquiños, Ó.; Shammakh, W. Projectile motion via Riemann-Liouville calculus. *Adv. Differ. Equ.* **2015**, *2015*, 1231. [CrossRef]
13. Alharbi, F.M.; Baleanu, D.; Ebaid, A. Physical properties of the projectile motion using the conformable derivative. *Chin. J. Phys.* **2019**, *58*, 18–28. [CrossRef]
14. Ebaid, A.; El-Zahar, E.R.; Aljohani, A.; Salah, B.; Krid, M.; Machado, J.T. Analysis of the two-dimensional fractional projectile motion in view of the experimental data. *Nonlinear Dyn.* **2019**, *97*, 1711–1720. [CrossRef]
15. Seddek, L.; Ebaid, A.; Aljohani, A.; Machado, J.A.T.; Baleanu, D. Re-Evaluating the Classical Falling Body Problem. *Mathematics* **2020**, *8*, 553. [CrossRef]
16. Spiegel, M.R. *Schaum's Outline of Theory and Problems of Theoretical Mechanics*; McGraw Hill: New York, NY, USA, 1967.
17. Poisson, E. *Advanced Mechanics*; Lecture Notes; Department of Physics, University of Guelph: Guelph, ON, Canada, 2008.
18. NASA Science. Solar System Exploration. Available online: https://solarsystem.nasa.gov/planets/overview/ (accessed on 27 September 2020).
19. Spiegel, M.R. *Laplac Transforms*; McGraw Hill: New York, NY, USA, 1965.